Title
LASER-BASED MULTIPARAMETER SYSTEM FOR AUTOMATIC SORTING OF MICROSCOPIC PARTICLES

Author
Turko, B.

Publication Date
1981-08-01

LBL-7520
Revised

Lawrence Berkeley Laboratory
UNIVERSITY OF CALIFORNIA

Engineering & Technical Services Division

Presented at the 1982 IEEE Nuclear Science Symposium, Washington, DC, October 19-22, 1982; and submitted for publication in IEEE Transactions in Nuclear Science

LASER-BASED MULTIPARAMETER SYSTEM FOR AUTOMATIC SORTING OF MICROSCOPIC PARTICLES

Bojan Turko and Branko Leskovar

August 1981

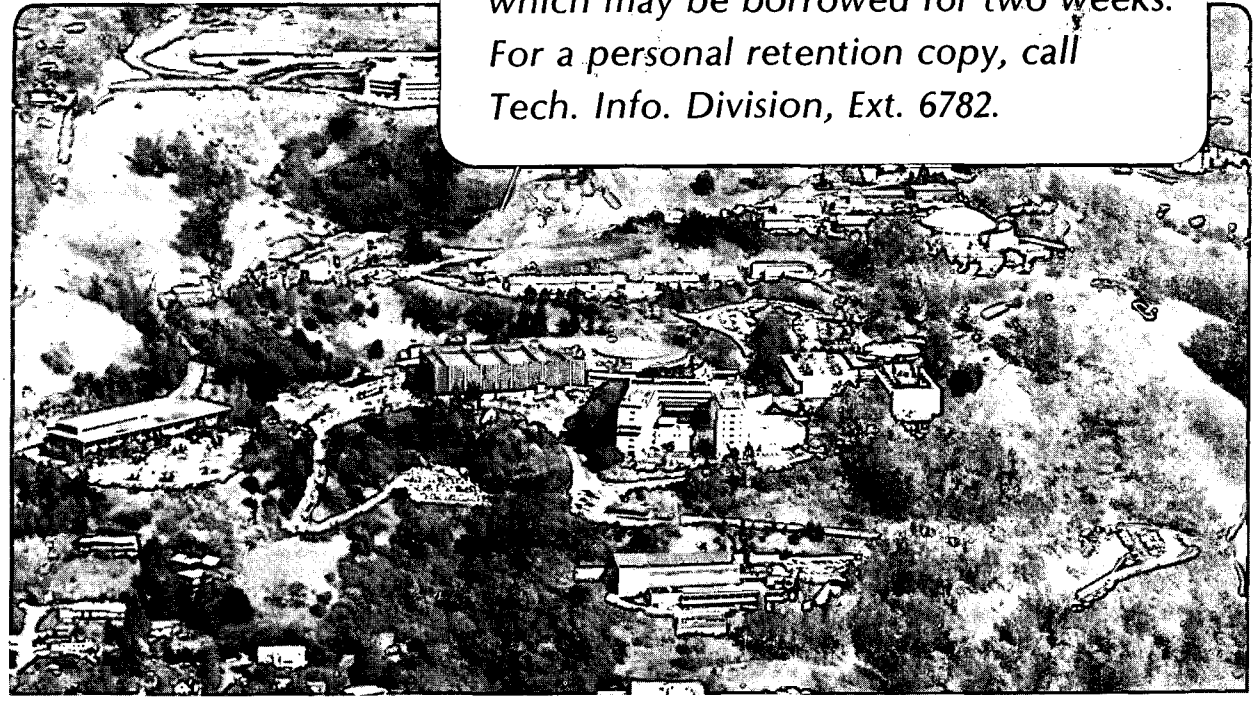

Prepared for the U.S. Department of Energy under Contract DE-AC03-76SF00098

LBL-7520 Rev.

DISCLAIMER

LASER-BASED MULTIPARAMETER SYSTEM FOR AUTOMATIC SORTING OF MICROSCOPIC PARTICLES

LBL-7520

Bojan Turko and Branko Leskovar

Lawrence Berkeley Laboratory
University of California
Berkeley, California 94720 USA

Abstract

The design, characteristics and experimental results of a Laser-Based Multiparameter system for automatically sorting microscopic particles are described. The system is used mostly for the analysis of biological cells which have been stained with fluorescent dyes and suspended in liquids. The cells, passing in single file through an elliptically focused laser beam, emit fluorescent signals, which are detected by sensors and processed, first in analog fashion and then digitally by a multichannel pulse-height analyzer. The two-color fluorescent and light scatter signals give certain parameters of the particles being measured. Sorting rates of several hundred per second are attainable. The high resolution and good stability of the system ensure fast, reliable and statistically meaningful measurement of particle populations.

Introduction

Numerous microscopic particle separators have been described in the Literature (Ref. 1-6). The system described here was mainly designed for the measurement of physical and biochemical properties of biological cells. The cell populations under test are first stained with fluorescent dyes. With proper dyeing and staining procedures, the cells will radiate fluorescence of the desired wavelength when made to pass one at a time through an elliptically shaped laser beam. Since the fluorescent decay time is very short, each cell radiates only during its passage through the beam. The amount of light radiated is a function of the stained volume of the cell. The intensity of the emitted light pulse is a function of the laser beam intensity and shape and also the cell velocity and shape. An optical system of lenses and filters separates each light pulse into its "red" and "green" components, focussing each onto the photocathode of the appropriate photomultiplier.

Current pulses proportional to the incident light are generated by the photomultipliers. A fast pulse preamplifier and charge integrator is used in pulse processing the signal. The integrator output is a voltage pulse whose amplitude is proportional to the total light collected during the passage of the cell through the laser beam. The preamplifier output shows the distribution of fluorescence emitted by a cell while it is crossing the beam. Since these signals are very similar to those found in the detecting charged particles in experimental nuclear physics, the instrumentation for analog and digital processing of the signals produced by fluorescent cells can be based on the experience gained in the nuclear field.

The cells cross the laser beam at random. The signal shaping and filtering requirements are similar to those in gamma-ray spectroscopy. Linear amplifiers designed for the optimum filtering of random pulses are used in cell signal processing. A multiparameter analog processing circuits was built for stretching the peaks of the shaped pulses along with the coincidence logic for the selection of desired categories of events. Also, analog signals proportional to the quotient of pairs of parameters are generated.

The selected signals can be digitized in either of two amplitude-to-digital converters and the results processed in a digital memory. All steps in the analog processing can be monitored on an oscilloscope. The digital processing of events can be also viewed with the aid of the memory monitor display. The results can then be transferred to the external central data processor, if first accepted by the operator.

Size of the particles can be determined by measuring forward scattered light as each one passes through the laser beam. This is done with a photodiode placed coaxially in the laser beam path to detect the forward scattered light. A beam dump in front of the diode absorbs all of direct light from the laser. An amplifier converts the photodiode current into a voltage pulse which gives an additional parameter for the analog signal processing.

The above system is made up of a number of optical, mechanical and electrical components. They are described and their function explained in the following text.

System Description

Most of mechanical and optical components of the system are mounted on a Newport Research Corporation optical table. This mechanically stable, vibration free base improves reliability and performance of the system. A diagram of the mechanical system, including the optics is shown in Fig. 1. The supporting electronic processing and control components of the system (Fig. 2) are housed in an adjacent rack. Modular components that do not have their own power supplies are housed in and powered by standard Nuclear Instrument Module (NIM) bins.

The light source for illuminating the stained cells in the flow chamber (Fig. 1) is a Spectra Physics Model 171-0 Ion laser with total output power of 10 W. The components of the laser system are the tunable laser head, a Model 270 Exciter, and a separate power meter. The strongest lines have wavelengths of 514.5 nm (3.7 W) and 488.0 (3.2 W). By employing UV additional optics, the laser can generate lines of 335.8 nm and 351.4 nm (0.07 W each).

The circular laser beam (1.6 mm diameter at 1/e points) is modified by beam shaping optics, consisting of two cylindrical lenses of 20 cm and 2 cm focal length, respectively. The beam passes through two windows and the center of the flow chamber. A beam dump in front of the exit window absorbs the emerging direct beam energy.

The stained cells cross the laser beam at the center of the flow chamber. The beam at this point has been shaped into an ellipse by the cylindrical lenses. The major axis is about 100 μm and the minor axis (oriented parallel with the cell flow) less than 10 μm. By adjusting the 20 mm lens the minor axis can

be focused at the point through which the stained cells pass. This minimum is about 7 μm wide, smaller than a typical cell diameter.

The flourescence emitted by excited cells is picked up at the two windows normal to the beam path. A microscope used for system alignment is placed in front of one window and the optical receiver at the other. A filter between the microscope and the flow chamber protects the viewer from scattered light. Water bubbles in the flow chamber might deflect whole beam into the microscope and cause eye damage if this filter were not used.

An F/1.6 lens at the optical receiver collects the fluorescent signal from the flow chamber. Behind the lens is a barrier filter which blocks the scattered light; this is followed by a dichroic interference filter which separates the fluorescence light into two colors. The red and green colors of the fluorescence light are thus separated and can be detected by two photomultipliers.

The shorter wavelength component passes through the dichroic mirror and a green barrier filter, and is focused by another F/1.6 projection lens onto a 260 μm pinhole. A collimating lens projects the light passing the pinhole onto the photocathode of the "green" photomultiplier. The red component of the fluorescence is reflected by the dichroic mirror and by a front surface mirror onto a third F/1.6 projection lens, which focuses the red light on another 260 μm pinhole. A red filter barrier ahead of the lens rejects shorter wavelengths, preventing any pick-up of the green components. In the compartment on the other side of each pinhole a collimating lens projects the light onto a photomultiplier. Both photomultipliers are RCA Model 4526.

A calibrating incandescent light is located in each photomultiplier compartment. The photomultiplier high voltage is turned off automatically when calibrating lights are turned on. The lights are brought directly in front of the pinholes when the calibrating lever is pressed. Images of the two illuminated pinholes, one red and the other green, are projected on the point in the flow chamber, where the fluorescing cells cross the laser beam. The micrometer which moves the surface mirrors should be adjusted until the two pinhole images intersect the moving stream of fluorescing cells. The laser beam, crossing the image horizontally, is also visible due to the Raman scattering in water. The point of proper alignment can be seen through the microscope, which can be swung into position in front of the viewing window in the flow chamber. In operation, the calibrating lights should be moved back to their rest position so as not to obstruct the optical paths between the pinholes and the photomultipliers.

The waveform of the output current at the collector electrode of the photomultiplier depends on the beam cross section and intensity, the shape of fluorescing cell and on its velocity. In a typical example, cells about 10 μm in diameter produce symmetrical pulses of 4 μs duration at half maximum (indicating a velocity of 2.5 m/s at the beam crossing).

Each photomultiplier output can be switched either to fast current-to voltage preamplifier, or to a charge integrating preamplifier (Fig. 1). Viewed on an oscilloscope, the output of the fast preamplifier shows the fine structure of the fluorescing part of the cell as it moves across the laser beam. The output of the integrating preamplifier shows a smooth pulse whose peak value is proportional to the total amount of light emitted during the cell passage, i.e. proportional to the stained portion of its volume. (A circuit diagram of the preamplifiers is shown in Fig. 3.)

The optical receiver assembly is mounted so as to be aligned with the flow chamber. The optimum position for the output can be found by an alignment procedure. Both the flow chamber and the optical receiver (except for the fast preamplifiers) were supplied by the Research Development Company, Los Alamos, New Mexico.

A steady stream of stained cells moves upwards, supported by a liquid in laminary flow sheath (distilled water free of air bubbles) in the flow chamber. The transport of the liquid sheath from the sheath reservoir to the waste reservoir through the flow chamber is controlled by a closely regulated vacuum system (Fig. 1). The system consists of a vacumm pump and a pump motor controlled by a vacuum regulating gauge. The stained cells, diluted in the sample cuvette, are brought to the flow chamber through a thin plastic tube and injected through a 100 μm orifice into the center of the liquid sheath. The diameter of the sample stream decreases as the cells move up through the flow chamber, forcing them into single file by the time they cross the beam. The adjustment of vacuum is critical since the slightest turbulence causes variations in the signal at the optical receiver, decreasing overall resolution of the measurement.

The mechanical flow control can change the sheath flow into a turbulent flow that effectively flushes out the flow chamber, eliminating accumulations of debris and air bubbles. Fluorescing debris suspended in sheath liquid can affect the measurement by increasing background signal in the photomultiplier. Air pockets may get stuck on the walls or windows of the flow chamber and cause laser beam defocusing or even a total deflection from its proper path.

The Analog Signal Processing

The analog processor, including four identical linear pulse peak stretcher channels with their associated logic, is shown in the block diagrams Figs. 4, 5 and 6. A positive voltage pulse at the input I_1 is transmitted to a discriminator LD_1 (LOWER DISCRIMINATOR) and a linear gate LG_1. Depending on the mode of operation selected, LG_1 will open at the appropriate time to pass the signal unchanged to the peak detector PD_1. There the highest point of the signal is stretched and is available at the output for the duration of the HOLD signal, defined by the logic. When the HOLD signal ceases, the stretcher is quickly discharged and initial conditions restored.

Each analog channel can operate either in an automatic mode or in a strobed (gated) mode. Also, any channel can serve as a master channel to the other channels and define coincident events in multiparameter signal processing. Three typical cases will be discussed for which the timing diagrams (not in scale) are shown in Figs. 7 to 9.

Single Channel Mode

Assume that only the first analog channel is used. A signal amplitude exceeding the threshold set by a potentiometer trips the lower discriminator LD_1. The Mode switch, which is assumed to be set in AUTO position, brings the logic "1" level to the gate G_{A1}. It is also assumed that a previous signal is not being processed at the time. The INHIBIT is in logic "0"

state, and because of the logic inversion at the input, G_{A1}, output is "1", enabling the gate G_{C1} after passing the logic OR_1 circuit. As soon as the lower discriminator (LD_1) fires, G_{C1} passes the logic level and sets the latch L_1, which in turn enables the peak detector PD_1 through the HOLD input. PD stretches and "memorizes" the peak of the input pulse and presents it to the output terminals.

The signal from L_1 passes OR_{21} (whose other input is set to zero by the mode switch in "IN" position) and coincidence circuit C, triggering SS_A, the first in a series of single shot multivibrators (SS_A to SS_G). The coincidence C was enabled because the three remaining inputs have been set to the logic "1" state. (It is assumed that the mode switches in the three unused channels were set to "OUT" position, passing the logic "1" signals through OR_{22}, OR_{23} and OR_{24} to C).

SS_A through SS_G (Fig. 4) generates a sequence of pulses used for both internal and external strobing, and provide also the inhibit and clear signals controlling the four channels. The sequence is as follows:

SS_A provides a continuously adjustable delay, followed by three fixed strobe pulses (SS_B, SS_D and SS_F) which are spaced by the intervals defined by SS_C and SS_E. SS_D and SS_F outputs are available as EARLY OUT and LATE OUT strobe signals on the front panel. They can be used, for instance, as coincidence signal for strobing the stretched linear signal into a multichannel Analog to Digital Converter (ADC). The timing sequence is shown in Fig. 7.

The end of the SS_F pulse triggers, through ORp, the dead time single shot SS_G. Dead times can be selected by a switch. The sum of SS_G and SS_H (through OR_C) generates a CLEAR signal to all latches and thus removes the HOLD signal from PD, causing a rapid discharge ofthe stretched pulse. The sum of SS_C to SS_G also provides an inhibit signal, that through G_{A1} and OR_1 closes G_{C1} and prevents acceptance of new events until the deadtime is over.

Coincidence Mode

Up to four linear channels can work simultaneously, constituting a four-parameter system for the selection of coincident events. The timing diagram in Fig. 8 shows a two-channel coincidence. The mode switches in the two unused channels should be in "GATED" and "OUT" positions respectively. In the two operating channels the mode switches should be set to "AUTO" and "IN" positions.

In either channel an input signal that exceeds the preset threshold level trips the lower discriminator and by opening the linear gate and setting the latch, stores the information in the peak detector as described earlier.

However, only if both events exceed the respective thresholds, will the latches L_1 and L_2 be set and start the sequence of pulses in the single shots SS_A to SS_G. If the two discriminators do not overlap, the program will not start and "RESET" single shot (SS_H) will be triggered via OR_R and G_R after the fired discriminator returns to zero (Fig. 4). SS_H will provide a CLEAR pulse through OR_C providing a fast discharge of the peak detector. Therefore, only a pair of events that occur simultaneously (i.e. whose discriminator crossings overlap) will produce a signal.

Gated Mode

Any of the four analog channels can be a master channel, operating as described in the Single Channel Mode Section. The mode selector switches of the master channel should be in "AUTO" and "IN" positions and those in the other channels in "GATED" and "OUT" positions.

An event exceeding the threshold in the master channel will be stored in its peak detector and start the sequence generator. The variable delay should be adjusted at the front panel controls so that a Delayed Strobe pulse is generated to be in coincidence with the peaks of the events entering the remaining channels. Illustrated in Fig. 9 are three possible cases. Only one event (input No. 2) is detected at its peak. The events at the Inputs No. 3 and No. 4 arrived too late and too early, respectively. This example shows the importance of making a proper adjustment of the delay and the strobe width.

Single Channel Analyzer Mode (SCA Mode)

Unwanted low-level events in any channel can be easily eliminated by raising the threshold level. In some measurements the events exceeding a desired level should also be eliminated. This can be accomplished either by using an external single channel analyzer (SCA), or using the built-in Upper Discriminator circuit.

External SCA Mode

The output from the selected pulse stretcher channel should be applied to an external Single Channel Analyzer (SCA) which will produce a logic output for each event that falls between the preset upper and lower discriminator levels. This output should be connected to the SCA IN terminal of the processor (Fig. 5). Provided that the selector is in EXT. position, the logic signal passes G_1 and OR_1, setting the latch L_1, which in turn enables the gate G_5. This gate is therefore open to pass the Late Strobe signal, which was generated by the processor in the course of the time sequence started by the same original event (Fig. 7). The signal is brought out as SCA OUT on the front panel of the processor and can be used as a gating pulse to the ADC which has the stretched signal of the same event waiting at its imput.

Internal SCA Mode

A built-in upper discriminator eliminates the need for an external Single Channel Analyzer (SCA). If the selector switch is in INT. position, each RESET pulse from the analog processor will pass G_2 and OR_1 (Fig. 5), setting the latch L_1 and thus enable G_5. When a Late Strobe pulse is generated (Fig. 7), it will pass G_5 and appear as a SCA OUT signal and open the gate to the external ADC. If the output of the selected linear channel is connected to the Upper Discriminator (UD) input, an event exceeding the preset threshold level will pass the logic signal from its output through G_3 and OR_2 and reset the latch L_1 closing G_5. Thus the gate G_5 will be already closed by the time the Late Strobe pulse arrives preventing SCA OUT signal from starting a conversion in the ADC.

Analog Divider

An independent analog divider has been included in the Analog Processor. Any peak detector output can be used as either numerator (Y_{IN}) or denominator (X_{IN}) input for the Analog Divider (Fig. 6). The output of the divider is a pulse whose amplitude

equals K (Y_{IN}/X_{IN}). K is a constant depending on which position is selected on gain selector switch namely, X1,X2 or X5. The linear quotient output can be digitized in the same way as the signal from the linear peak detector channels. The early Strobe Output of the Analog Processor should be used for the gating of the ADC by the same gating procedure described under Internal SCA Mode.

Linear Gate

In order to make the system more versatile, a linear gate is included in the analog processor (Fig. 4). An analog signal will pass from the input to the output of the gate only when enabled by either early or late, internally generated strobe pulse. Any event, that is coincident with the operation of the analog channels of the processor, is thus allowed to appear at the output of the gate.

Circuit diagrams of the analog processor are shown in Figs. 10 through 14. The experimenter can choose which one of the numerous combinations of parameters to use. A typical setting is for the two-color fluorometry of the stained cells, shown in Fig. 15. Each color is digitized separately. The selection of live displays (normal, contour and isometric) makes it easier to interpret the results.

A Tektronix RM 15 oscilloscope and an ORTEC, Inc. Model 449-2 LOG/LIN Ratemeter are included in the system (Fig. 2). The amplifier and the Analog Processor outputs can be checked and continually monitored by the oscilloscope, and the ratemeter measures event rates at the selected output. Also, two high voltage regulated power supplies for the photomultiplier, and the pinhole light power source are housed in the same rack, as the power switches, the vacuum gauge and the computer interface modules.

Processing of Digitized Events

Two 1024-channel amplitude-to-digital converters (Northern Mod. NS-622) and a 4094-channel digital analyzer (Northern Mod. NS-636) offer sufficient resolution and data storage capacity for most purposes (Fig. 2). Often much less resolution is quite acceptable in sorting out the stained cell populations. The memory can be divided in 65 separately addresssable subgroups of 64 channels each. Therefore, a number of samples can be quickly analyzed and compared on the instant playback display. Either ADC has access to the analyzer through a data selector, which also provides simultaneous access to both ADC's for two-dimensional data analysis (64 x 64 channels). Three display modes can be selected for better viewing. The two ADC's provide X and Y address and the number of events can be recorded along the Z-axis.

Transfer of data from the digital analyzer to a remote data processor is done in two steps. The first is from a NS-636 to a LBL built Σ-2 Interface Module followed by a Data Transmission System Users Terminal Module (Fig. 2). Both modules were provided by the LBL Chemical Biodynamics Division.

Experimental Results

The system was primarily designed for flow cytofluorometry studies at the Lawrence Berkeley Laboratory Chemical Biodynamics Division. The instrument has been used continuously for a period of several years. The performance of this system and its extensive application in the cellular biology experiments has been described in a number of published works (Ref. 7-21). A typical example is shown in Fig. 16 where changes in a cell population over a period of several days are shown as a series of spectra. A two-dimensional presentation of another cell population in the Fig. 17 shows the end result of the two-color microfluorometry. Two channels of the system's analog processor in coincidence mode were used for the selection of the events. X and Y axis represent the intensity of each parameter and the vertical axis the number of events.

Appendix

Principal parts of the systems and their characteristics are listed below:

Light Source

A Spectra Physics Mod. 171-0 Ion Laser with Mod. 270 power Supply and Mod. 170 Power Meter is used. With the standard optics the laser can deliver a total of 10 W. The tunable wavelengths (nm) and corresponding power (W) are: 514.5 (3.7); 501.7 (0.5); 496.5 (1.0); 488.0 (3.2); 476.5 (1.2) and 457.9 (0.5). Additional lines are available with U.V. optic attached: 363.8 (0.07) and 351.1 (0.07).

The Flow Chamber and Control Box

They were made by Research Developments Inc., Los Alamos, New Mexico as described in Ref. 2.

Beam Shaping Optics

Two quartz cylindrical lenses (20 cm and 2 cm focal lengths respectively), each mounted on a Newport Corporation micromanipulator consisting of a tilt table, support post and translation stage.

Two Color Optical Receiver

They were also made by Research Developments Inc., Los Alamos, New Mexico. Principal components of the receiver are a F/1.6 collimating lens, a barrier filter, a dichroic mirror, "green" and "red" barrier filters, and a 260 μm pinhole and a F/1.6 collimating lens for each optical channel. Two RCA 4526 photomultipliers are used for fluorescence detection. The receivers each contain a fast preamplifier and an integrating preamplifier (Fig. 3).

Vacuum Pump

A Cole-Parmer Instrument Co., (Chicago) Masterflex pump, motor and controller is used. The controller is slightly modified for remote control by the pressure gauge.

Vacuum Regulator

Dwyer Instruments, Inc., Michigan City, Indiana Photohelic Pressure Switch/Gauge is located in the adjacent rack. The vacuum sensing tube connects the gauge with the waste reservoir. The pressure range is up to 20 psig. Proper pressure for turbulence free operation of the flow chamber has to be found experimentally.

Optical Table

The laser, the beam focusing system, the flow chamber and the optical receiver are mounted on a Newport Corporation (Fountain Vallejo, Calif.), optical table. Stable, reproducible operation of the system, free-of-shocks and noise typical in most environments is obtained.

Amplifiers

Two Ortec Model 450 Research Amplifiers are used, one in each channel of the optical receiver. The gain of each amplifier can be varied from 2.5 through 3000. Independent active low-pass and high-pass filtering can be adjusted by selecting time constants from 0.1 to 10 μs both for integrate and differentiate modes.

High Voltage Power Supply

Two Ortec Model 456 High Voltage Power Supplies provide regulated high voltage for the photomultipliers in the optical receiver. They are housed in an AC powered NIM bin . A High Voltage Time Control Switch (Fig. 2) makes sure that the high voltage is disconnected when pinhole light for the alignment of the optical receiver is turned on. Damage of the photomultipliers may result if the photomultipliers are exposed to too much light when the high voltage is applied.

Ratemeter

An Ortec Model 449 Ratemeter is used for monitoring the event rates appearing at the outputs of the analog processor. Change of the event rates can be viewed on the ratemeter's dial. An audible sound proportional to the rate is also generated as a warning signal to the experimenter.

Four Parameter Analog Processor

This unit was built by the LBL Electronics Research and Development Group and is described in the Analog Signal Processing section of this text.

Analog-to Digital Converter

Two identical Northern Scientific Model NS-622 Analog-To-Digital Converters are used for the simultaneous conversion of any two parameters. Maximum number of channels is 1024. The resolution can be reduced by a five step switch down to 64 channels.

Memory Unit

A Northern Scientific Model 636 Memory System is used for on-line data processing and storage. The 4092 channel memory can be divided into up to 64 subgroups that are individually accessible. Each memory section can store an individual spectrum. Two-dimensional storage and display is possible when the two ADCs are used simultaneously, along with the analog processor. Isometric, contour or profile display mode can be selected. A choice of linear or logarithmic data presentation on the CRT is available. Either parallel or serial data transfer to the external processor is possible.

Data Interface

The system is used in the LBL Chemical Biodynamics Division. Two LBL-built NIM modules are used for interfacing the Division's internal computer system. The modules are Data Transmission System Users Terminal (LBL No. 16 x 3221) and NS636 to Σ-2 Interface.

Acknowledgements

This work was performed as part of the program of the Electronics Research and Development group of the Lawrence Berkeley Laboratory and supported by the National Cancer Institute and the U.S. Department of Energy under contract DE-AC03-76SF00098.

Reference to a company or product name does not imply approval or recommendation of the product by the University of California or the U.S. Department of Energy to the exclusion of others that may be suitable.

References

1. Holm, D.M., and Cram, C.S., "An Improved Flow Microfluorometer for Rapid Measurement of Cell Fluorescence, Experimental Cell Research 80, pp. 105-110, 1972.

2. Steinkamp, J.A., Fulwyler, M.J., Coulter, J.R., Hiebert, R.D., Horney, J.L., and Mullaney, P.F., "A New Multiparameter Separator for Microscopic Particles and Biological Cells", Review of Scientific Instruments, Vol, 44, No. 9, pp. 1301-1310, September, 1973.

3. Van Dilla, M.A., Steinmetz, L.L., Davis, D.T. Colvert, R.N. and Grey, J.W., "High Speed Cell Analysis and Sorting in the Flow Systems: Biological Applications and New Approaches", IEEE Trans. on Nucl. Sci. NS-21, No. 1, pp. 714-720, February, 1974.

4. Kim, M., Khosrow Bahrami, and Kwang B. Woo, "A Discrete-Time Model for Cell-Age, Size, and DNA Distributions of Proliferating Cells, and its Application to the Movement of the Labeled Cohort", IEEE Trans. on Biomed. Engineering, BME-21, No. 5, pp. 387-398, September, 1974.

5. Steinkamp, J.A., Hansen, K.M., Crissman, H.A., "Flow, Microfluorometric and Light-Scatter Measurement of Nuclear and Cytoplasmic Size in Mammal Cells", The Journal of Histochemistry and Cytochemistry, Vol. 24, No. 1, pp. 292-297, 1976.

6. Sharpless, T.K., and Melamed, M.R., "Estimation of Cell Size From Pulse Shape in Flow Cytofluorometry", The Journal of Histochemistry and Cytochemistry, Vol. 24, pp. 257-264, No. 1, 1976.

7. Bartholomew, J.C., Yokota, H., and Ross, P., "Effects of Serum on the Growth of Balb 3T3 A31 Mouse Fibroblast and an SV40-Transformed Derivative", J. Cell Physiol. Vol. 88, pp. 277-286, 1976.

8. Bartholomew, J.C., Neff, N.T., and Ross, P., "Stimulation of WI-38 Cell Cycle Transit: Effect of Serum Concentration and Cell Density", J. Cell Physiol. Vol. 89, pp. 251-258, 1976.

9. Teng, M., Bartholomew, J.C., and Bissell, M.J., "Insulin Effect on the Cell Cycle: Analysis of the Kinetics of Growth Parameters in Confluent Chick Cells", Proc. Natl. Acad. Sci., Vol. 73, pp. 3173-3177, 1976.

10. Hawkes, S.P. and Bartholomew, J.C., "Quantitative Determination of Transformed Cells in a Mixed Population by Simultaneous Fluorescence Analysis of Cell Surface and DNA in Individual Cells", Proc. Natl. Acad. Sci., Vol. 74, pp. 1626-1630, 1977.

11. Teng, M.H., Bartholomew, J.C., and Bissell, M.J., "Synergism Between Anti-Microtubule Agents and Growth Stimulants in Enhancement of Cell Cycle Traverse", Nature, 268, pp. 793-841, 1977.

12. Wade, C.G., Baker, D.E., and Bartholomew, J.C., "Selective Fluorescence Quenching of Benzo (a) pyrene and a Mutagenic Diol Expoxide in Mouse Cells", Biochem., 17, pp. 4332-4337, 1978.

13. Becker, J.F., and Bartholomew, J.C., "Aryl Hydrocarbon Hydroxylase Induction in Mouse Liver Cells in Culture", Chemico-Biol. Inter., 26, pp. 257-266, 1979.

14. Wade, C.G., Rhyne, R.H., Woodruff, W.H., Bloch, D.P., and Bartholomew, J.C., "Spectra of Cells in Flow Cytometry Using a Vidcon Detector", J. Histochem. and Cytochem., 27, pp. 1049-1052, 1979.

15. Bartholomew, J.C., Pearlman, A.L., Landolph, J.R., and Straub, K., "Modulation of the Cell Cycle of Cultured Mouse Liver Cells by Benzo(a) pyrene and Derivatives", Cancer Res., 29, pp. 2538-2543, 1979.

16. Greasey, A.A., Bartholomew, J.C., and Merigan, T.C., "Role of GoG1 Arrest in the Inhibition of Tumor Cell Growth by Interferon", Proc. Natl. Acad. Sci., 77, pp. 1471-1475, 1980.

17. Peterson, J.A., Bartholomew, J.C., Stampfer, M., and Ceriani, R., "Analysis of Expression of Human Mammary Epithelial Antigens in Normal and Malignant Breast Cells at the Single Cell Level by Flow Cytofluorimetry", Exptl. Cell Biol., 49, 1-14, 1981.

18. Parry, G., Bartholomew, J.C., and Bissell, M.J., "Growth Regulation in RSV Infected Chicken Embryo Fibroblasts: The Role of the Src", Gene Nature 288, 720-722, 1980.

19. Bartholomew, J.C., Hughes, A., and Das, K., "Alterations in DNA Synthesis in Mouse Liver Cells Caused by the Tumor Promoter 12-O-Tetra decanoylphorbol-13-Acetate (TPA)", J. Supramolecular Structure. In press.

20. Cohen, S.R., Burkholder, D.E., Varga, J.M., Carter, M., and Bartholomew, J.C., "Cell Cycle Analysis of Cultured Mammalian Cells After Exposure to 4, 5, 8-Trimethylpsoralen and Long-Wave Ultraviolet Light", J. of Investigative Dermatology, 76, pp. 409-413, 1981.

21. Greasey, A.A. Bartholomew, J.C., and Merigan, T.C., "Direct Evidence for Interferon's Site of Action in the Cell Cycle", Exptl. Cell Res. In press.

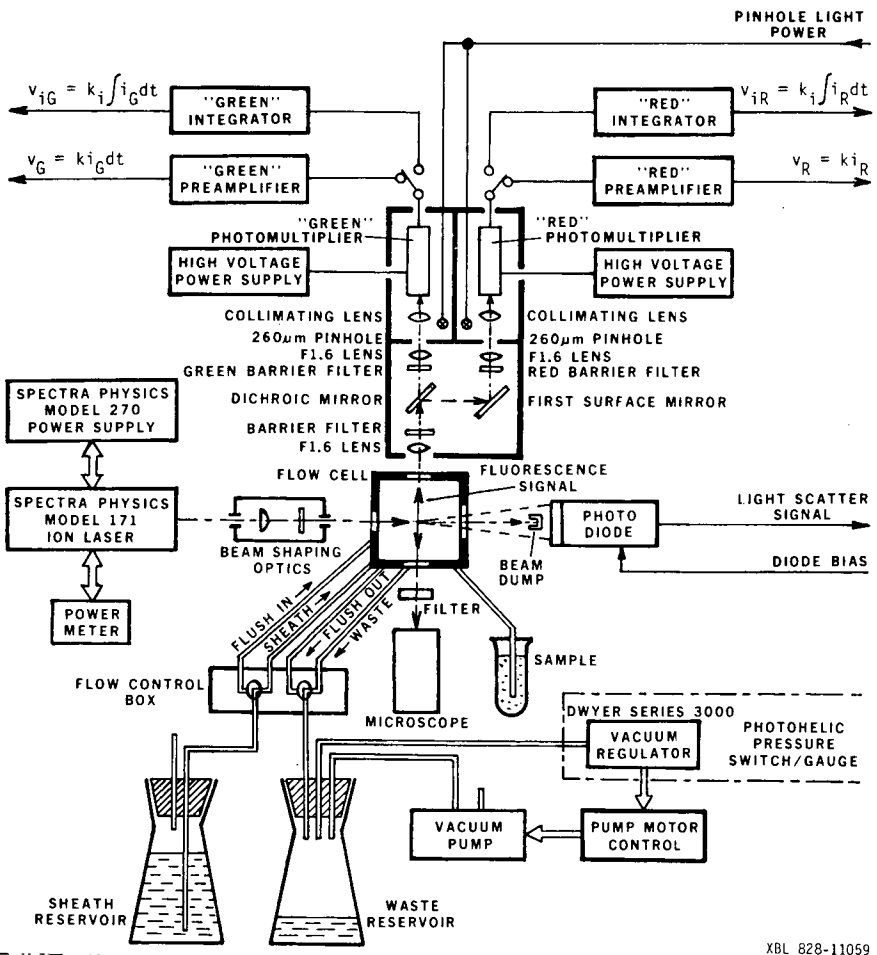

Fig. 1 Laser-based multiparameter system for automatic sorting of microscopic particles: General block diagram.

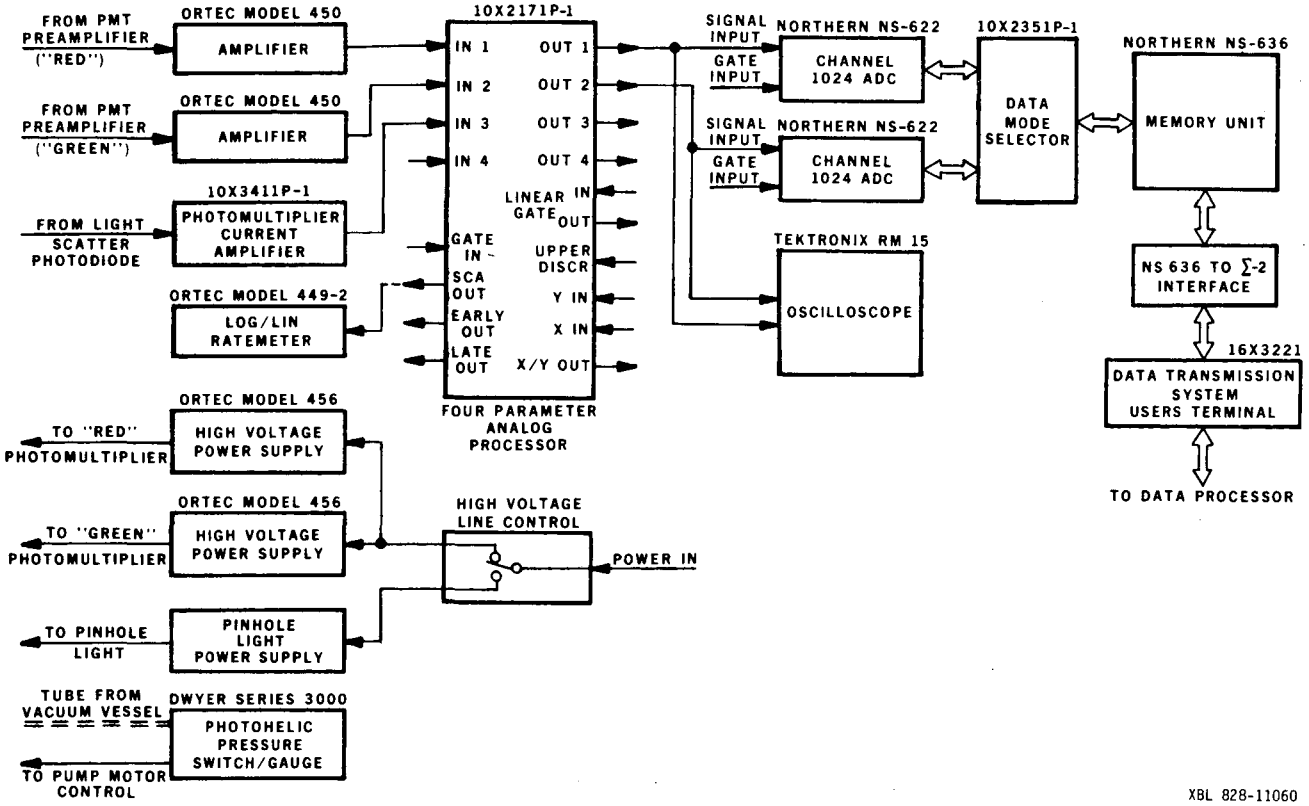

Fig. 2 Electronic component block diagram of the system.

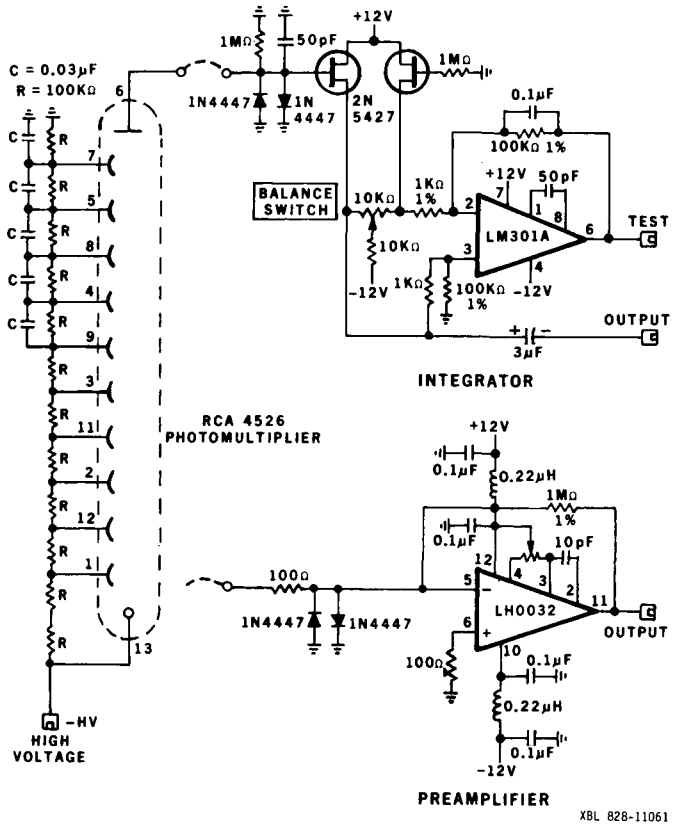

Fig. 3 Optical receiver photomultiplier, fast preamplifier and integrator circuit diagram.

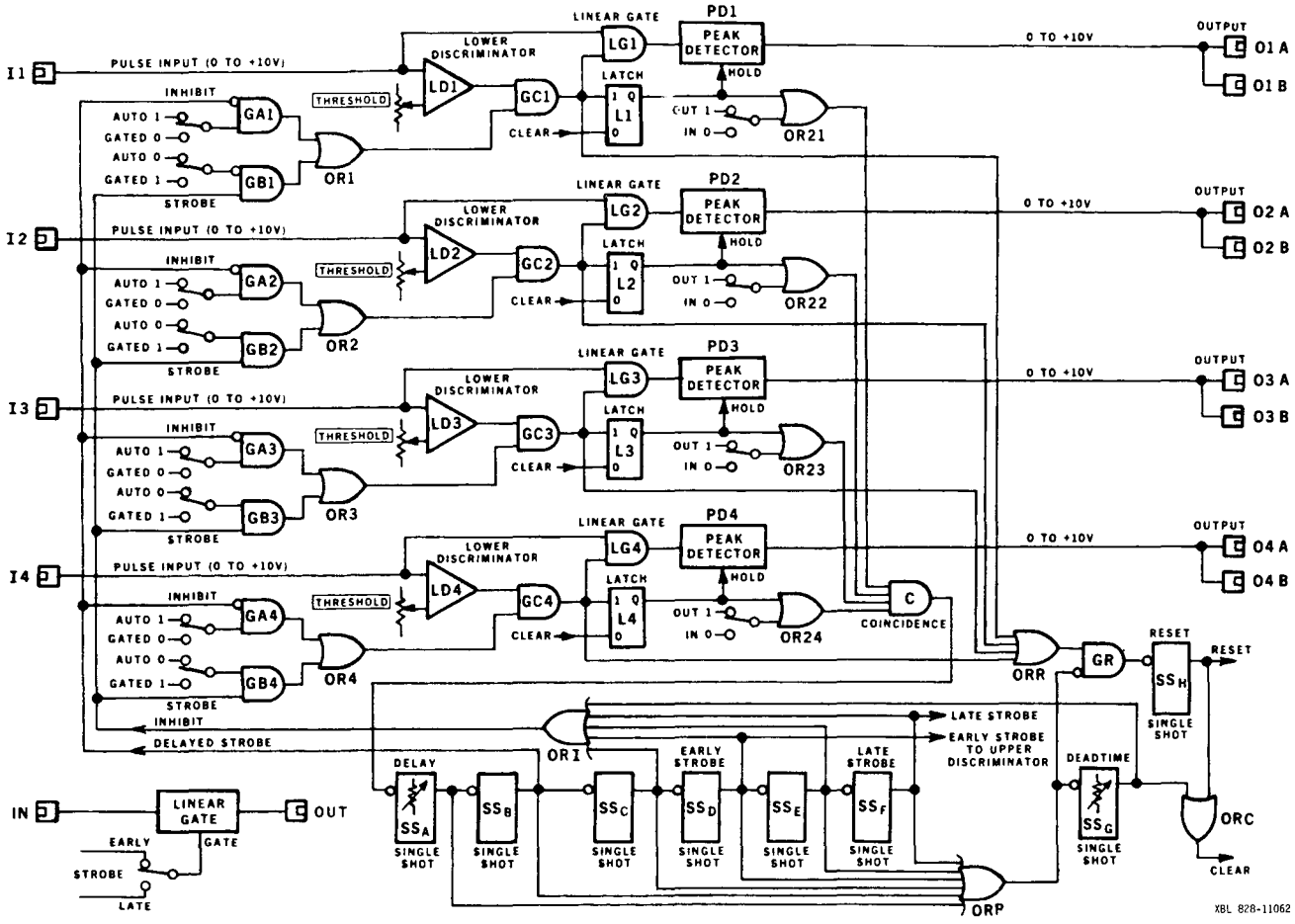

Fig. 4 Four parameter analog processor module block diagram (discriminator, stretchers and logic).

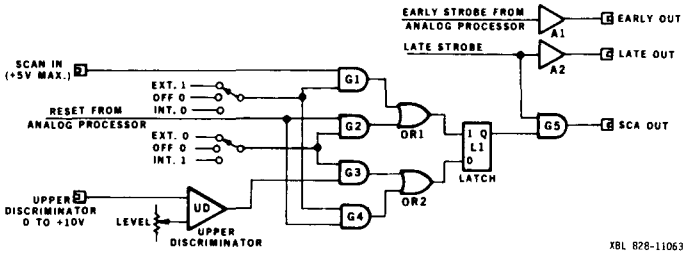

Fig. 5 Four parameter analog processor module block diagram (upper discriminator).

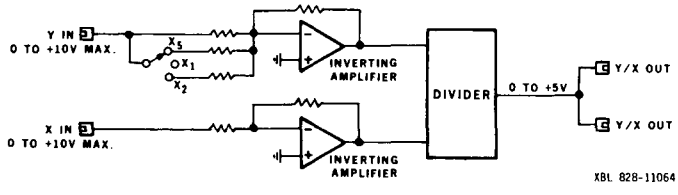

Fig. 6 Four parameter analog processor module block diagram (analog divider).

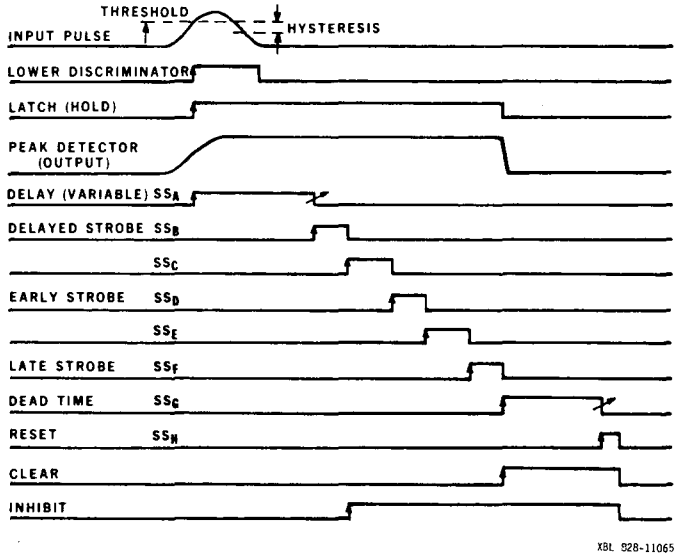

Fig. 7 Single channel mode timing diagram.

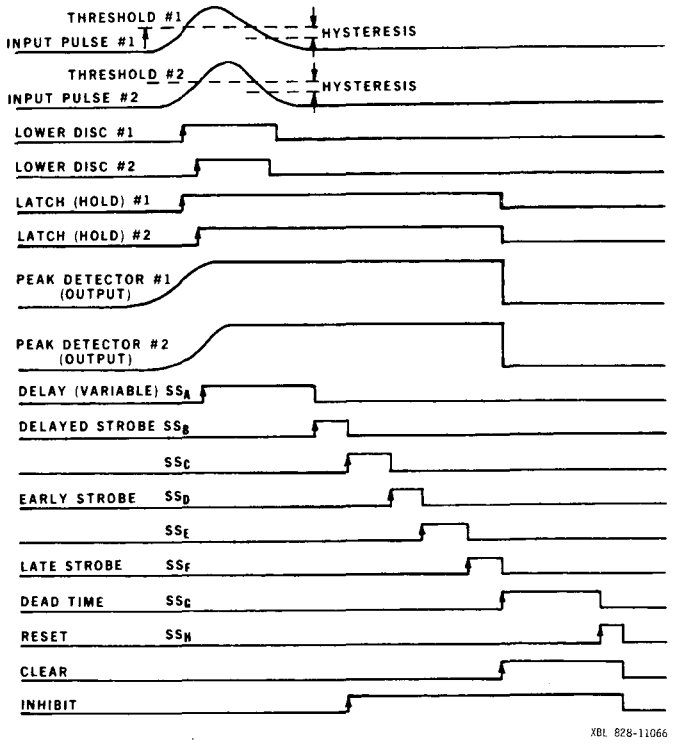

Fig. 8 Coincidence mode timing diagram.

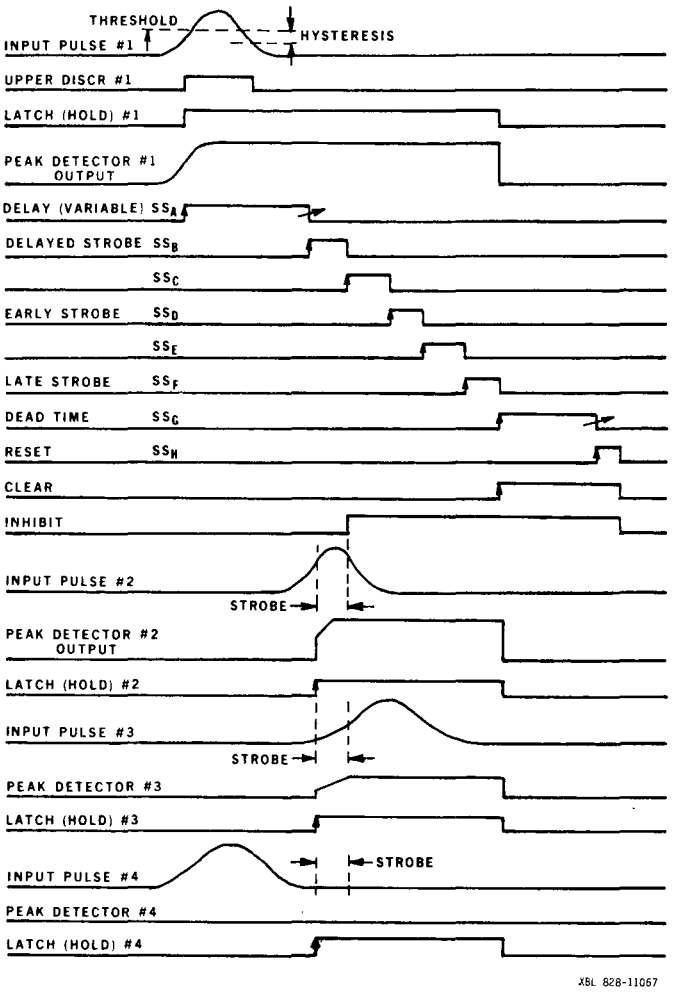

Fig. 9 Gated mode timing diagram.

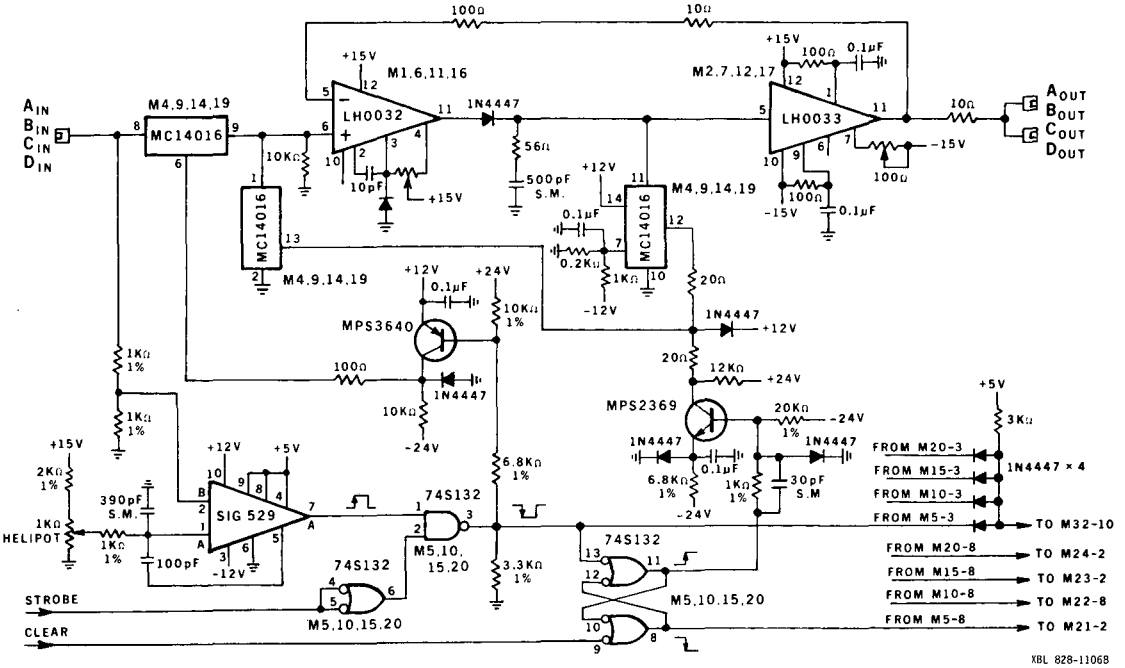

Fig. 10 Peak detector and lower discriminator circuit diagram.

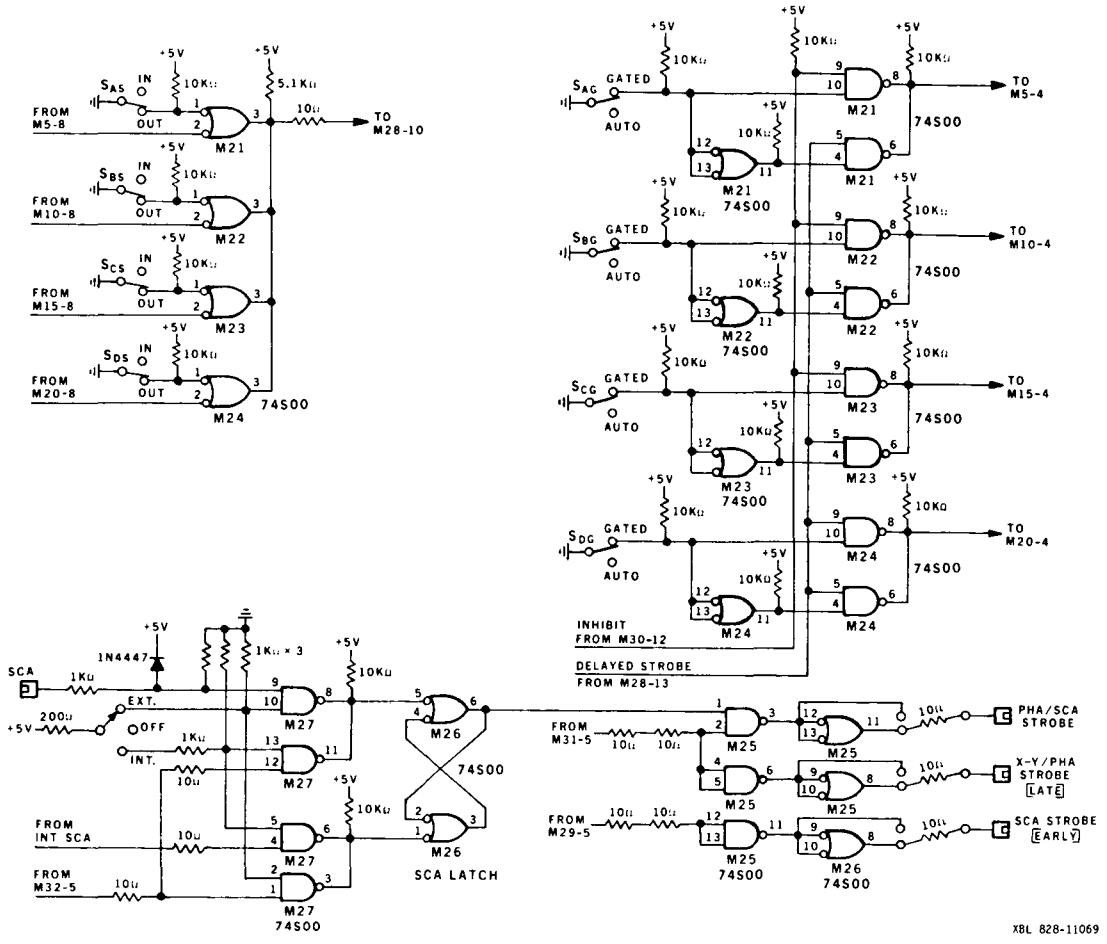

Fig. 11 Mode selection circuit diagram.

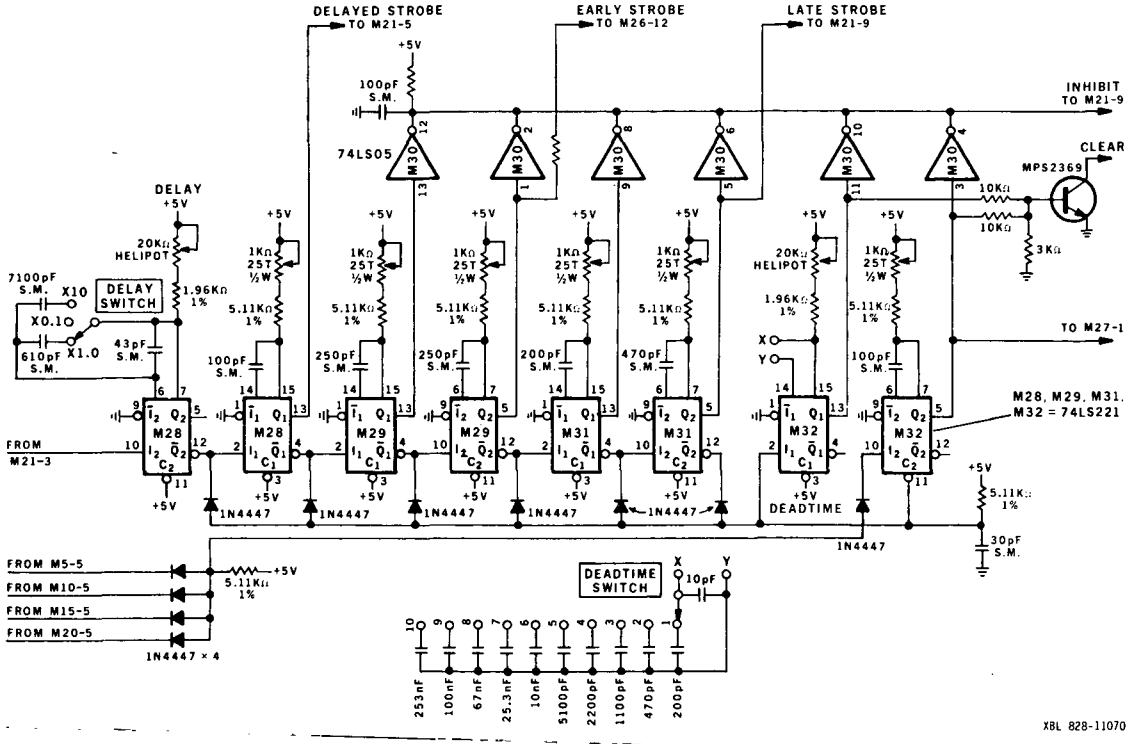

Fig. 12 Time sequence circuit diagram.

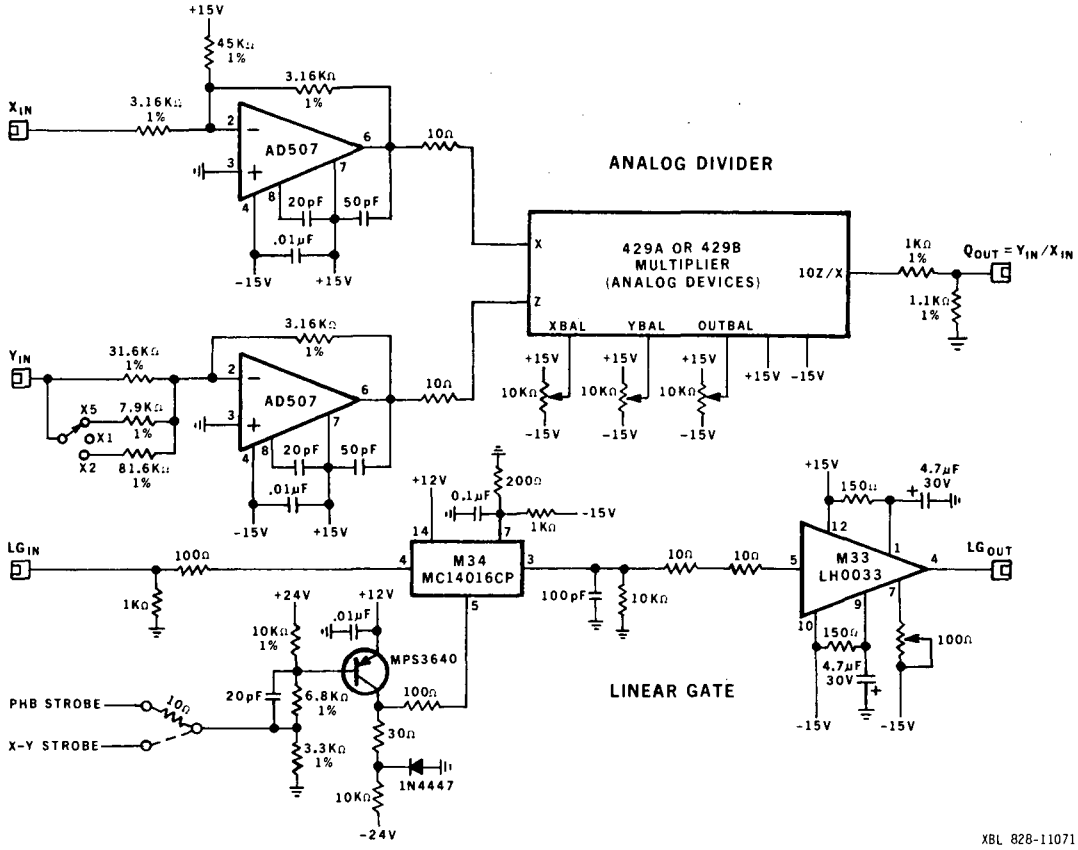

Fig. 13 Analog divider and linear gate circuit diagram.

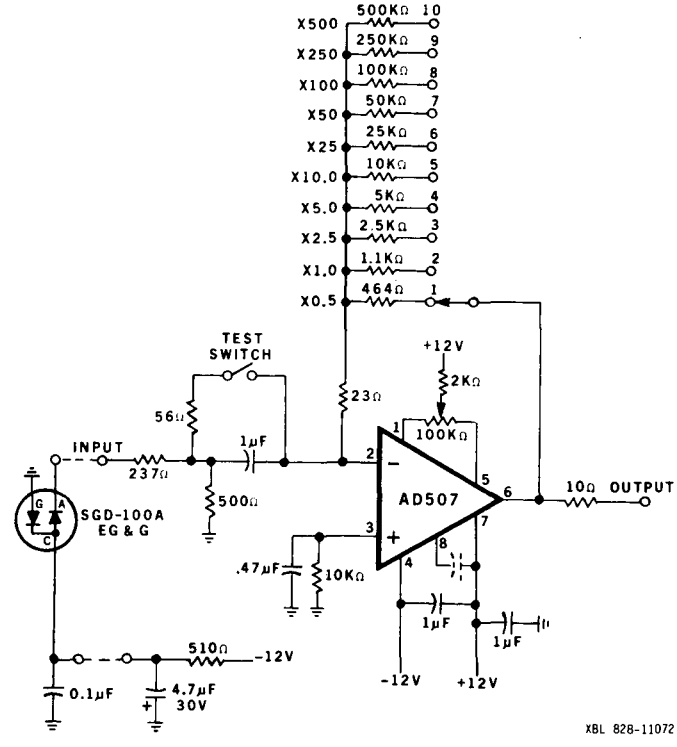

Fig. 14 Light scatter photodiode current amplifier.

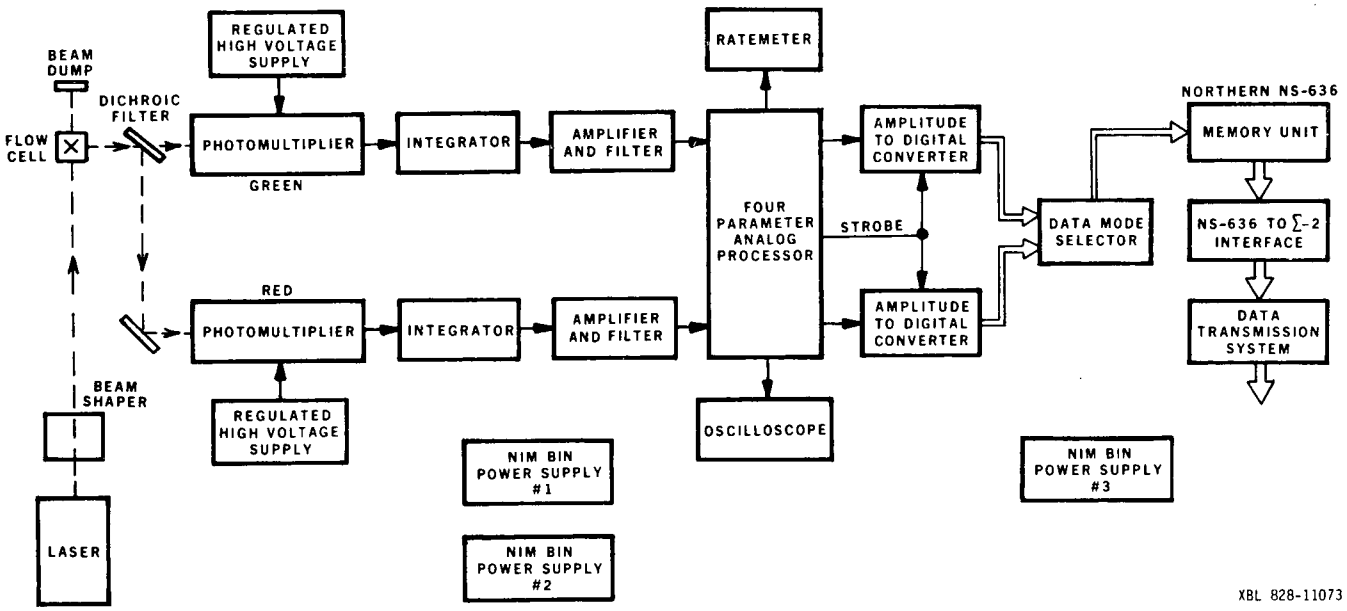

Fig. 15 Typical system set-up for two-color flow microfluorometry.

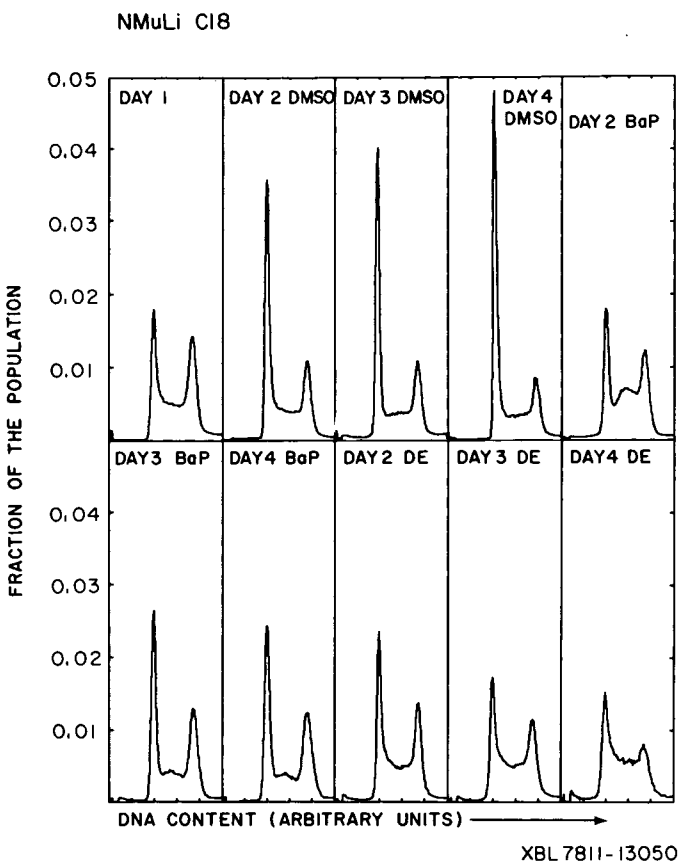

Fig. 16 Spectra of the changes in a cell population for a period of several days (Courtesy of J. Bartholomew, LBL Chemical Biodynamics Division)

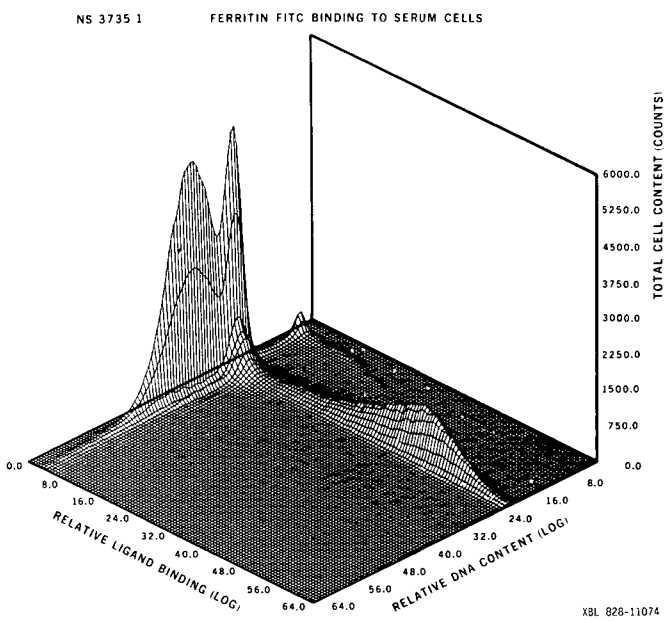

Fig. 17 Two-dimensional distribution of a cell population. Two-color optical receiver and the analog processor in coincidence mode was used (Courtesy of J. Bartholomew, LBL Chemical Biodynamics Division)

This report was done with support from the Department of Energy. Any conclusions or opinions expressed in this report represent solely those of the author(s) and not necessarily those of The Regents of the University of California, the Lawrence Berkeley Laboratory or the Department of Energy.

Reference to a company or product name does not imply approval or recommendation of the product by the University of California or the U.S. Department of Energy to the exclusion of others that may be suitable.

TECHNICAL INFORMATION DEPARTMENT
LAWRENCE BERKELEY LABORATORY
UNIVERSITY OF CALIFORNIA
BERKELEY, CALIFORNIA 94720